# Resonant light-controlled self-assembly of ordered nanostructures

V.V. Slabko [a,*], A.S. Tsipotan [a], A.S. Aleksandrovsky [a,b]

[a] Siberian Federal University, Russian Federation
[b] L.V. Kirensky Institute of Physics, Russian Federation

## Abstract

The possibility of light-controllable formation of heterogeneous nanostructures containing resonant metallic and semiconductor nanoparticles is considered. Interaction energy between light-induced dipole polarization of nanoparticles at modest light intensity can be much more than the thermal motion energy. The configuration of self-assembled nanostructure can be controlled by the frequency and polarization of the light.
© 2012 Elsevier B.V. All rights reserved.

## 1. Introduction

Construction of nanoscale objects, as well as the study of their properties and of their applications for new devices of electronics and photonics are presently among the main trends of both fundamental and applied scientific research. The use of self-organization phenomena is attractive since it can be the basis of relatively cheap technology for production of complex nanoscale objects. Employment of laser irradiation of nanoparticles produces various effects that are known to lead to the assembly of nanoparticles into whether disordered or ordered structures. For instance, mesoscale filaments of carbon and gold nanoparticles are irreversibly obtained under laser irradiation using optical trapping, hydro-thermal and chemical effects [1]. Light-controlled assembly of CdTe nanoparticles in helical structures [2] was ascribed to production of photogenerated charges. Another prospective approach implies the modification of potential energy of the particles in the non-resonant electromagnetic field of the light wave due to particle interactions [3]. Self-assembly of nanoparticles under action of non-resonant electromagnetic field with the frequencies in the wide range up to the optical ones was also investigated in [4]. When nanoparticles resonantly interact with the electromagnetic field, this interaction gives new opportunities for selective action upon them [5]. It was theoretically shown that, in case of plasmon-resonant metallic nanoparticles, the action of electro-magnetic field with proper frequency must influence geometry of the produced structures [6]. It was found in [6] that interaction of particles in the laser field leads to the shift of their resonant frequencies, and this shift depends on the distance between particles and mutual orientation of the particles with respect to the laser field polarization. The given configuration of the aggregate of particles can be obtained only when laser field induces their attraction, and the latter requires proper choice of the frequency and polarization of laser field.

The selectivity between different geometries of nanostructures must be strongly dependent on the

---

* Corresponding author.
  *E-mail address:* slabko@iph.krasn.ru (V.V. Slabko).

resonance linewidth of individual nanoparticle. Since plasmon resonances of metallic nanoparticles are rather wide, it is interesting to consider the light-controlled aggregation of nanoparticles which possess narrower resonances. Such resonances can be found whether in semiconducting nanoparticles [7,8] or in doped dielectric nanoparticles [9]. On the other hand, the formation of heterogeneous nanostructures composed of different materials usable for electronics, namely, dielectric or semiconductor nanoparticles as well as conducting ones, is of greater interest. Principal difference of such a system is the presence of several resonances with non-coinciding frequencies and linewidths. In the present paper we consider resonant light-controlled effects on formation of nanostructures that contain whether both semiconductor and metal nanoparticles or exclusively semiconductor ones.

## 2. Calculation model

When metal or semiconductor nanoparticles in the state of Brownian motion interact with laser field, then electric dipole polarization is induced on them. Interaction of this polarization with laser field results in optical trapping in the regions with the dimensions of order of wavelength. Increased density of nanoparticles results in increased aggregation rate within an optical trap. Aggregates produced are commonly disordered on the nanoscale, but can bear the signs of ordering on the sub-wavelength scale due to a variety of processes depending on the medium containing nanoparticles [1,10]. When several particles in the course of Brownian motion occasionally appear closely enough to each other, then their polarizations interact each other. This is one of manifestations of near-field effects. If energy of electromagnetic interaction between nanoparticles exceeds the energy of thermal motion kT and the energy of a barrier preventing the aggregation then irreversible formation of nanostructures will happen. Let us consider an ensemble of $N$ nanoparticles with coordinates $r_i$ and interacting each other through their polarization induced by laser field. The dimensions of an ensemble are supposed to be much less than the wavelength. Then external field strength can be considered homogeneous within the ensemble. Then electric field strength is considered to depend only on time: $\mathbf{E} = 1/2\mathbf{E_0}\exp(i\omega t) + $ c.c. Local field acting on every nanoparticle is a sum of external field and the fields induced by all the rest particles. In the dipole–dipole interaction approximation, the dipole moment vector at the frequency $\omega$ induced on $i$th particle is:

$$\mathbf{d}_i = \chi_{0i}\left(\mathbf{E} + \sum_{j \neq i}\mathbf{E}_j\right),\tag{1}$$

Here $\chi_{0i} = |P_{12}|_i^2/\hbar(\Omega + i\Gamma_i)$ is linear polarizability of isolated nanoparticle, $|P_{12}|_i^2$ is an electric dipole matrix element for the transition from ground to the excited state of particle, $\Omega = \omega_{0i} - \omega$ is the resonance detuning, $\hbar$ is the Planck constant, $\Gamma_i$ is the homogeneous width of the transition, and $\mathbf{E}_j$ is the field produced by $j$th nanoparticle in the position of $i$th particle [11]:

$$\mathbf{E}_j = \frac{3(\mathbf{d}_i\mathbf{r}_{ij}) - \mathbf{d}_i r_{ij}^2}{r_{ij}^5},\tag{2}$$

where $r_{ij} = r_i - r_j$ is the distance between particles. Interaction energy of $i$th and $j$th particles with excited dipole polarization will be [12]:

$$W_{d_{ij}} = \frac{(\mathbf{d}_i\mathbf{d}_j)r_{ij}^2 - 3(\mathbf{d}_i\mathbf{r}_{ij})(\mathbf{d}_j\mathbf{r}_{ij})}{r_{ij}^5},\tag{3}$$

Calculation of interaction energy between particles, therefore, requires solution of the system of $N$ equations with dipole moments of every particle defined by expression (1). Also, renormalised linear polarizability of every particle $\hat{\chi}_i$ can be obtained, that is in general case a tensor connecting dipole moment vector induced on $i$th particle with the electric field strength vector: $\mathbf{d}_i = \hat{\chi}_i\mathbf{E}$. Imaginary part of renormalized polarizability determines the absorption of light by $i$th particle.

Consider the binary interaction of two particles with different resonant frequencies in a dipole approximation. As an example let us choose a nanoparticle of silver [11] and semiconductor nanoparticle of CdSe [7,8]; optical properties of these nanoparticles are well studied.

Using (1) and introducing $p_i = |P_{12}|_i^2/\hbar r^3$, we obtain expressions for $x$ ($x\|r_{12}$) and $y$ ($y \perp r_{12}$) components of dipole moments of a pair of nanoparticles:

$$
\begin{aligned}
d_{1x} &= E\cos\alpha \cdot \frac{r^3 p_1(\Omega_2 + 2p_2 + i\Gamma_2)}{(\omega_1^x - \omega)(\omega_2^x - \omega) + i(\Omega_2\Gamma_1 + \Omega_1\Gamma_2)},\\[4pt]
d_{2x} &= E\cos\alpha \cdot \frac{r^3 p_2(\Omega_1 + 2p_1 + i\Gamma_1)}{(\omega_1^x - \omega)(\omega_2^x - \omega) + i(\Omega_2\Gamma_1 + \Omega_1\Gamma_2)},\\[4pt]
d_{1y} &= E\cos\alpha \cdot \frac{r^3 p_1(\Omega_2 - p_2 + i\Gamma_2)}{(\omega_1^y - \omega)(\omega_2^y - \omega) + i(\Omega_2\Gamma_1 + \Omega_1\Gamma_2)},\\[4pt]
d_{2y} &= E\cos\alpha \cdot \frac{r^3 p_2(\Omega_1 - p_1 + i\Gamma_1)}{(\omega_1^y - \omega)(\omega_2^y - \omega) + i(\Omega_2\Gamma_1 + \Omega_1\Gamma_2)}
\end{aligned}
\tag{4}
$$

where $\omega_{1,2}^x$ and $\omega_{1,2}^y$ are resonant frequencies for $x$ and $y$ components of dipole moment, $\alpha$ is the angle between the line connecting the centers of the nanoparticles and the vector $E$ (Fig. 1):

$$\omega_{1,2}^x = \frac{1}{2}(\omega_{01} + \omega_{02})$$
$$\pm \sqrt{\frac{1}{4}(\omega_{01} + \omega_{02})^2 - \omega_{01}\omega_{02} + 4p_1p_2 + \Gamma_1\Gamma_2},$$

$$\omega_{1,2}^y = \frac{1}{2}(\omega_{01} + \omega_{02})$$
$$\pm \sqrt{\frac{1}{4}(\omega_{01} + \omega_{02})^2 - \omega_{01}\omega_{02} + p_1p_2 + \Gamma_1\Gamma_2}$$

Dependence of imaginary part $(d_{1x} + d_{2x})/E \cos \alpha$ $(d_{1y} + d_{2y})/E \sin \alpha$ on the external field wavelength, that is responsible for the absorption of the whole system, consisting of two particles, is plotted in Fig. 1 (solid line) for $x$ (a) and $y$ (b) components of electromagnetic field, correspondingly.

Using expressions (3) and (4) the two-particle dipole–dipole interaction energy averaged over the period of optical oscillations can be expressed as:

$$W = \frac{d_{01y}d_{02y}\cos(\phi_{d1}^y - \phi_{d2}^y) - 3d_{01x}d_{02x}\cos(\phi_{d1}^x - \phi_{d2}^x)}{4r^3},$$
(5)

where $d_{01y}$, $d_{02y}$, $d_{01x}$, and $d_{02x}$ are modules and $\phi_{d1}^y, \phi_{d2}^y, \phi_{d1}^x$, and $\phi_{d2}^x$ are the phases of dipole moments of the first and the second particles.
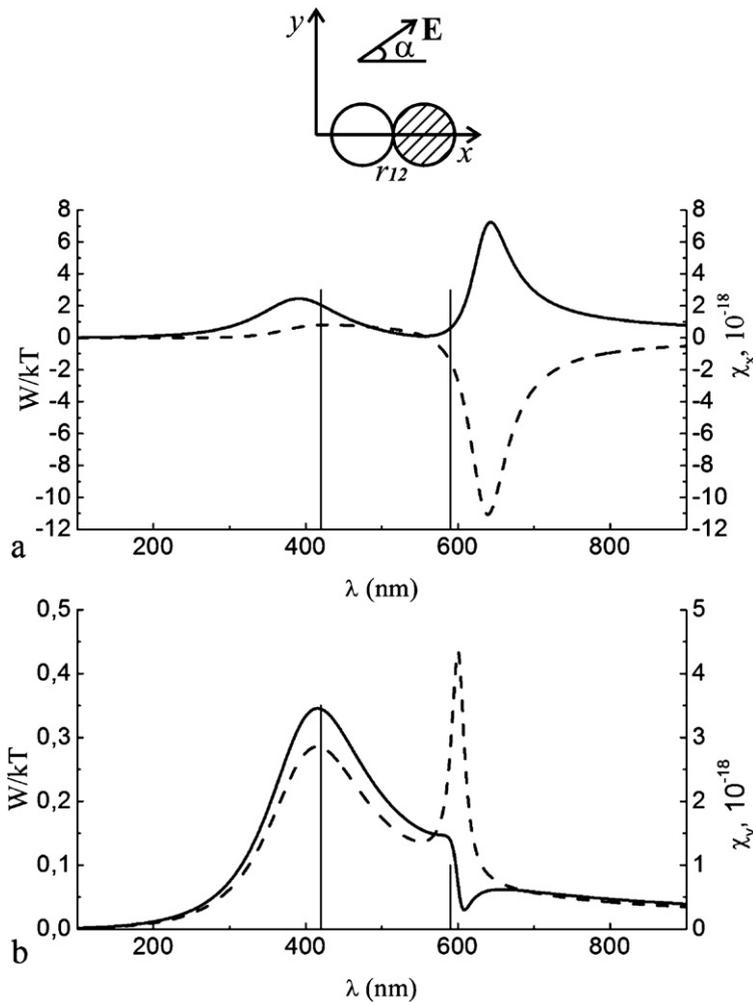


Fig. 1. Wavelength dependence of imaginary part of polarizability for pair of nanoparticles (solid line) $\chi$ and normalized dipole–dipole interaction energy of particles (dashed line). Vertical lines are resonant wavelengths of non-interacting nanoparticles. External field is directed at (a) $\alpha = 0°$ and (b) $\alpha = 90°$.

## 3. Results and discussion

### 3.1. One metallic and one semiconductor particles

Dependencies of dipole–dipole interaction energy normalized on room temperature thermal energy kT, on the laser wavelength are plotted in Fig. 1 (dashed lines), for angles $\alpha = 0°$ (Fig. 1a) and $\alpha = 90°$ (Fig. 1b). Following parameters were used in the calculation:

for semiconducting CdSe nanoparticle we will take into account only most prominent long-wavelength exciton transition with resonant wavelength corresponding to $\omega_{01}$ being equal to $\lambda_{01} = 590$ nm, the linewidth $\Delta\lambda_1 = 3$ nm, the radius $R_1 = 5$ nm and dipole moment of the transition $|P_{12}|_1^2 = 1.91 \times 10^{-31}$ erg cm$^3$ [7,8];
for silver nanoparticle corresponding values are $\lambda_{02} = 420$ nm, $\Delta\lambda_2 = 90$ nm, $R_2 = 6$ nm, $|P_{12}|_2^2 = 3.12 \times 10^{-30}$ erg cm$^3$ [11];
external field strength equals to $E = 200$ ESU ($10^6$ W/cm$^2$), and temperature of the medium equals to $T = 300$ K;
distance between particles $r_{12} = 13$ nm.

As can be seen from expression (4) and Fig. 1, wavelength dependence of imaginary part of susceptibility responsible for the absorption noticeably differs from that for non-interacting particles, both for field components $x$ and $y$. $x$ component has two prominent maxima with the positions shifted from centers of non-perturbed resonances. This shift is due to the particle interaction and depends on the resonances widths $\Gamma_1$ and $\Gamma_2$, resonant frequencies of non-interacted particles and electric dipole moments of transitions $|P_{12}|_1^2$ and $|P_{12}|_2^2$. Characteristic feature is the existence of a dip in the area of 600 nm for imaginary part of polarizability for $y$ field component (Fig. 1b). This dip is a Fano-like resonance and reflects interference nature of the interaction of pair of particles with differing resonant frequencies and linewidths [13,14]. Spectral dependence of nanoparticles interaction energy at $\alpha = 0°$ has a potential well (Fig. 1a dashed line) with the depth considerably exceeding the thermal motion energy. If the height of potential barrier hindering the aggregation is smaller than this depth, the formation of stable pair of nanoparticles becomes possible. This pair of particles will be oriented at the angle $\alpha = 0°$ relatively to vector. Its stability can be due to whether van der Waals or Coulomb forces, the latter arising from electron transfer between semiconductor quantum dot and metallic nanoparticle [15]. Similar dependence at $\alpha = 90°$ also

has the minimum (Fig. 1b), but minimal energy remains positive in this case.

### 3.2. Three particles

Let us further consider the formation of the structures containing three or more nanoparticles, for instance, two metallic and one semiconducting particles (latter are shown by dashed circles) (Fig. 2), two semiconducting and one metallic particles (Fig. 3), and three semiconducting particles (Figs. 6 and 7). We will suppose that particles 1 and 2, as denoted by $r_{12}$ label, are already in post-aggregated state. Analytical solution of Eqs. (1) and (2) for three particles, that allows to calculate dipole–dipole interaction energy in the process of adjoining of the third particle with respect to the first ones at the pre-given angle $\theta$, and to
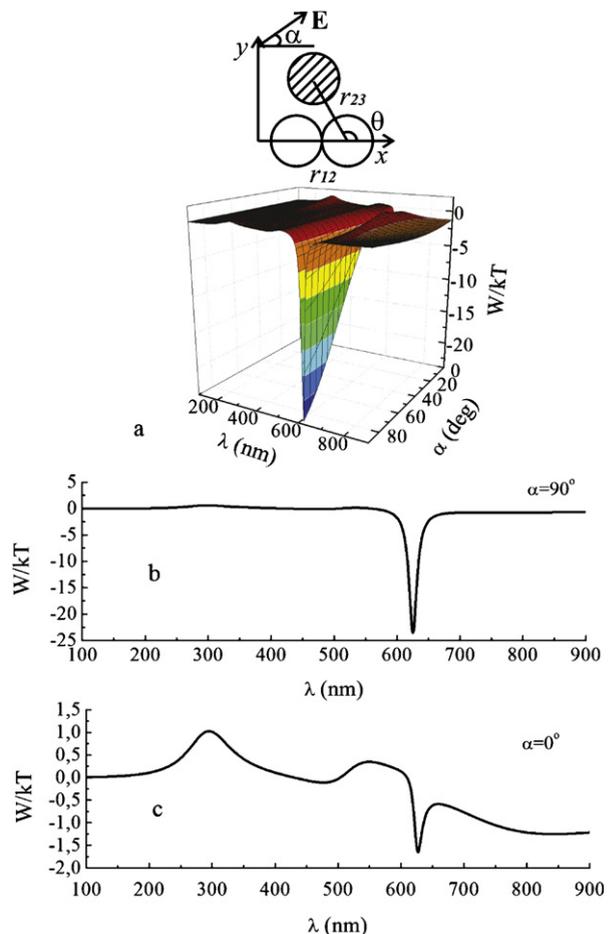


Fig. 2. (a) 3D dependence of normalized dipole–dipole interaction energy of two metallic and one semiconducting particles on the laser wavelength and electric field direction angle. (b) Section of 3D dependence by $\alpha = 90°$ plane. (c) Section of 3D dependence by $\alpha = 0°$ plane.

determine the depth, spectral and angular position ($\alpha$) of potential well is very cumbersome and is not presented here. Graphic results are presented in Figs. 2a–c and 3a–c. Particle parameters are the same are quoted above, $r_{12} = R_1 + R_2$, and distance between the second and the third particles was $r_{23} = 13$nm, the angle $\theta$ between vectors $r_{12}$ and $r_{23}$ was chosen to be $120°$. Value of $r_{23}$ is taken to be larger than the sum or particle radii, in order to account for possible residual thickness of organic molecule layers commonly used for preventing fast uncontrolled aggregation. Polarization of external field is directed at the angle $\alpha$ to the direction $x$ between particles 1 and 2.

As seen in Fig. 2b and c, potential well at $\alpha = 90°$ has the depth 23.5 kT, while at $\alpha = 0°$ the depth is 1.65 kT. Consequently, for chosen parameters of the system, the stable position of the third particle at room temperature is easier achievable when external field is directed at $\alpha = 90°$ (Fig. 2b). Spectral width of potential well at 625 nm approximately corresponds to the absorption spectrum of semiconductor particle. At $\alpha = 0°$ two minima of interaction energy exist at 476 and 626 nm (Fig. 2c). Potential well depth at 476 nm is 0.1 kT that is insufficient for formation of stable structure. Widths of the first and second minima approximately correspond to extinction spectra of metallic and semiconductor particles, correspondingly.

Results for the case of two semiconductor and one metallic particles somehow differ (Fig. 3). Potential well depths at 670 nm are sufficient for stable structure formation both for $\alpha = 90°$ (Fig. 3b) and for $\alpha = 0°$ (Fig. 3c). At the wavelength 479 nm one more potential well exists (Fig. 3b) with the depth of order of 0.95 kT.

Calculations for different configurations of nanoparticles in a nanostructure, that is, for different values of angle $\theta$, show that not all of them are equally controllable via choice of wavelength, laser intensity
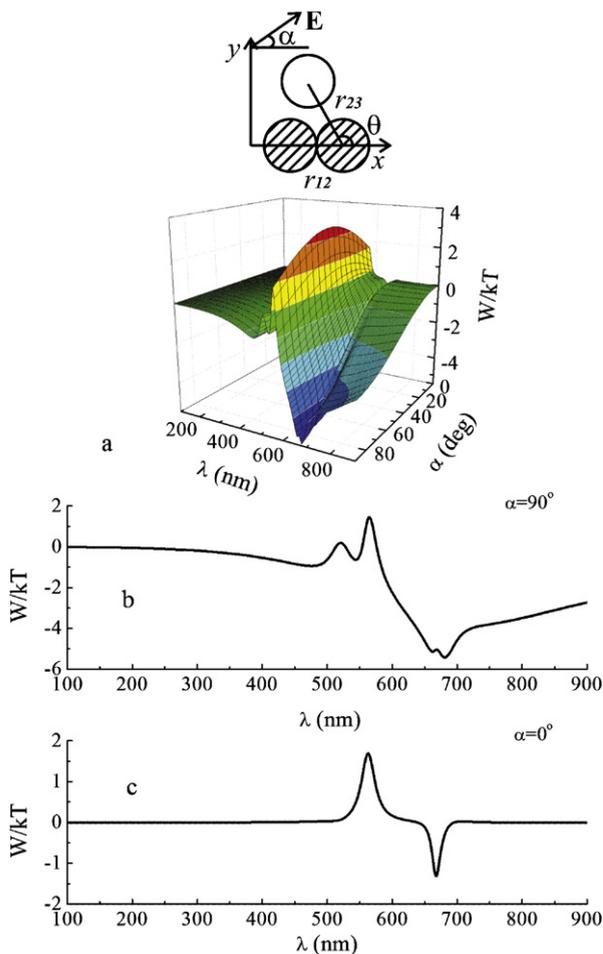


Fig. 3. (a) 3D dependence of normalized dipole–dipole interaction energy of two semiconducting and one metallic particles on the laser wavelength and electric field direction angle. (b) Section of 3D dependence by $\alpha = 90°$ plane. (c) Section of 3D dependence by $\alpha = 0°$ plane.
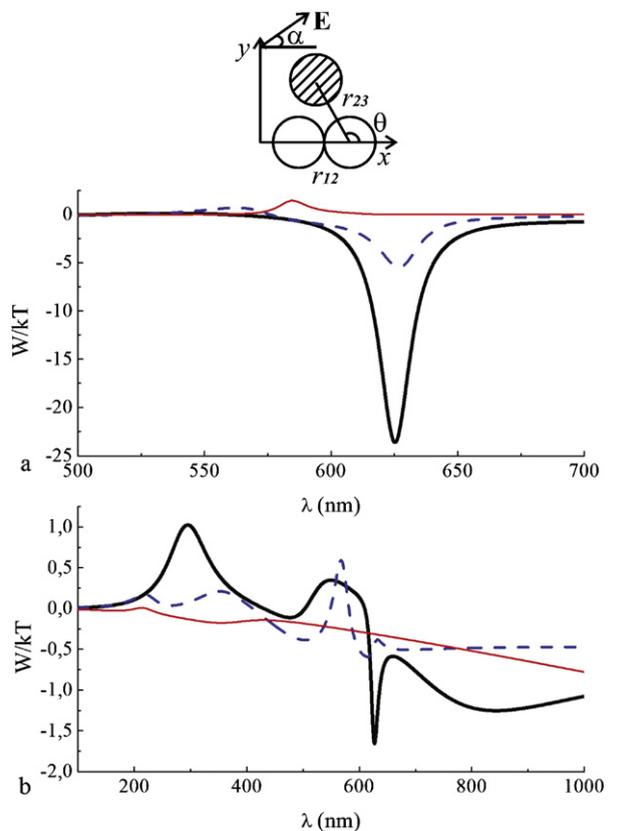


Fig. 4. Normalized dipole–dipole interaction energy of two metallic and one semiconducting particles on the laser wavelength for different configurations of the nanostructure, $\theta = 120°$ (thick solid), $90°$ (dash), and $0°$ (thin solid): (a) $\alpha = 90°$ and (b) $\alpha = 0°$.

and polarization. For instance, in case of two metallic and one semiconductor particles and $\alpha = 0°$ (Fig. 4b) variation of $\theta$ from $120°$ to smaller values leads to decrease of potential well depth, but its spectral position varies within several nm, that is smaller than the spectral width of the potential well. This means that selective formation of $\theta = 120°$ configuration is possible via proper choice of laser intensity, while other configurations cannot be controlled. For $\alpha = 90°$ (Fig. 4a) the configuration with $\theta = 120°$ is the best controllable, again, but that with $\theta = 90°$ can be preferably obtained, too, by the tuning the wavelength to 550 nm and proper choice of intensity. Oppositely, for two semiconductor and one metallic particles (Fig. 5), the best controllable configuration is $\theta = 0°$ at $\alpha = 0°$ with the potential well depth more than 20 kT at the wavelength required 678 nm. For $\alpha = 90°$ the configuration with $\theta = 120°$ requires the laser wavelength 680 nm, while $\theta = 90°$ requires wavelength choice 600 nm for best selectivity.

For comparison, let us compare results for heterogeneous structures with the case of homogeneous structure formation in the process of adjoining the semiconductor particle to a pair of already aggregated semiconductor particles. Fig. 6 presents the general view of interaction energy dependence on the laser wavelength and $\alpha$ angle for $\theta = 120°$. Individual resonant frequency of every aggregated particle is chosen to be corresponding to the wavelength 590 nm, while for the third particle it corresponds to 510 nm, in accordance with the particle radius $r_3 = 3$ nm. Linewidths of isolated nanoparticles and laser field strength are the same as in previous calculations. As can be seen from Fig. 6, two potential wells exist at $\alpha = 90°$ and $\alpha = 20°$ with corresponding depths 63 kT and 43 kT at wavelengths 595 nm and 655 nm. Fig. 7a and b depicts the sections of 3D dependence at $\alpha = 0°$ and $\alpha = 90°$ for different $\theta$ angles. For $\alpha = 90°$ selective formation of whether $\theta = 120°$ configurations (at the recommended wavelength 593 nm) or $\theta = 90°$ configurations (at 554 nm) is possible, while suitable potential wells for $\theta = 0°$ and $\theta = 45°$ are absent. When laser field polarization angle $\alpha = 0°$, selective formation of configurations with $\theta = 120°$, $90°$, $45°$ and $0°$ becomes
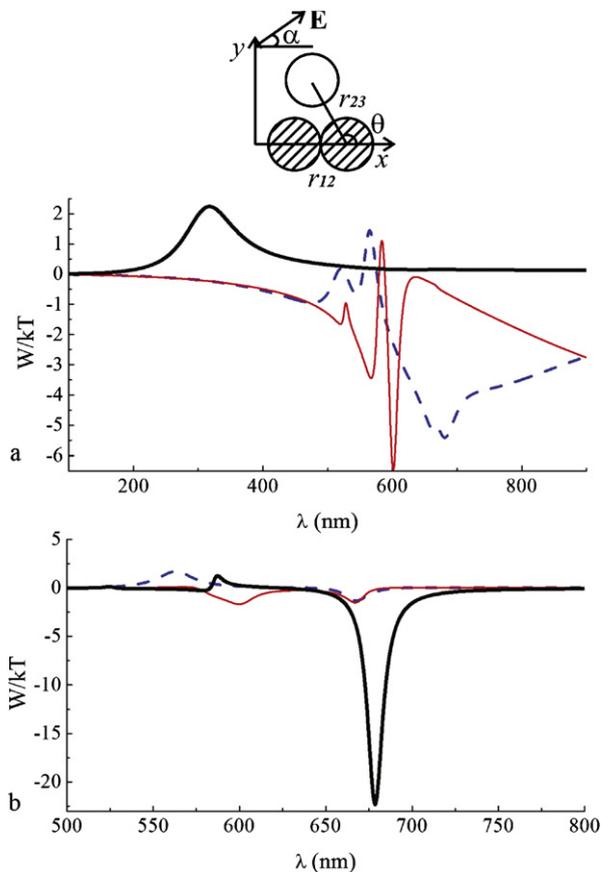


Fig. 5. Normalized dipole–dipole interaction energy of two semiconducting and one metallic particles on the laser wavelength for different configurations of the nanostructure: $\theta = 120°$ (dash), $90°$ (thin solid), and $0°$ (thick solid): (a) $\alpha = 90°$ and (b) $\alpha = 0°$.
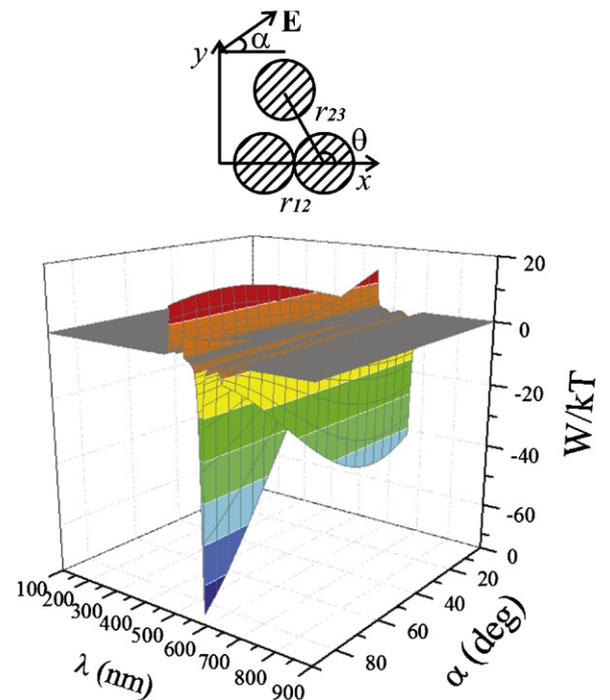


Fig. 6. 3D dependence of normalized dipole–dipole interaction energy of the semiconducting particle adjoining the pair of aggregated semiconducting particles on the laser wavelength and electric field direction angle.
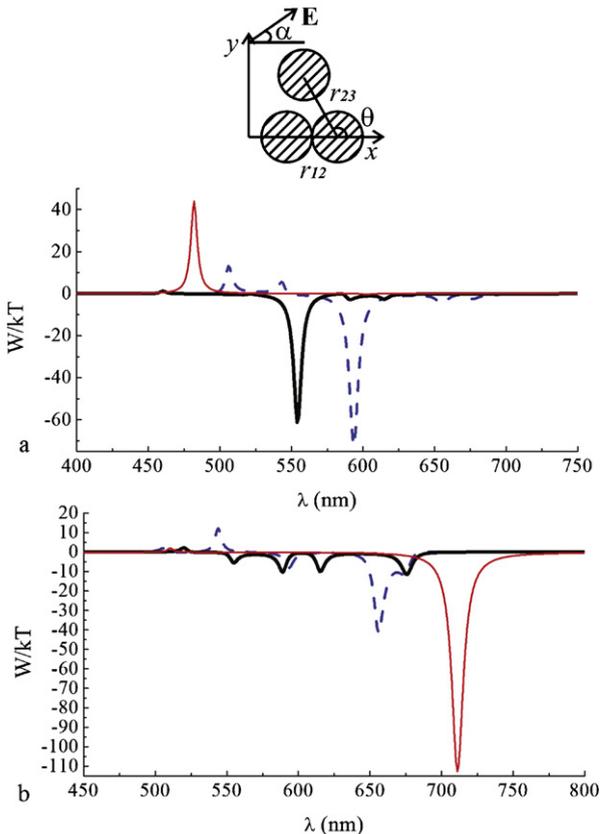
Fig. 7. Normalized dipole–dipole interaction energy of semiconductor particle in the vicinity of two aggregated semiconducting particles on the laser wavelength for different configurations of the nanostructure: $\theta = 120°$ (dash), $90°$ (thick solid), and $0°$ (thin solid): (a) $\alpha = 90°$ and (b) $\alpha = 0°$.
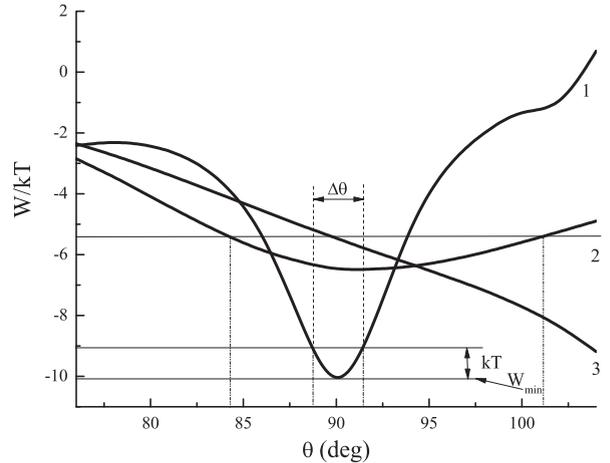


Fig. 8. Dependence of potential energy of interaction on the angle $\theta$ for $\alpha = 90°$. 1, three semiconducting nanoparticles; 2, two semiconducting and one metallic nanoparticles; 3, two metallic and one semiconducting nanoparticles.

$\theta_0$. This dependence is presented in Fig. 8 for three different sets of particles. The laser wavelengths for every set are chosen from Figs. 4, 5 and 7 as the positions of potential minima. The possibility to build selectively the structure with desired configuration ($\theta_0$) can be quantitatively described by finding the angular width $\Delta\theta$ of the potential well on the level that is 1 kT higher than the value of potential well minimum. Evidently, $\Delta\theta$ can characterize the angular selectivity of desirable structure in the conditions of thermodynamic equilibrium with the ambient medium. As can be found from Fig. 8, for $\theta_0 = 90°$ $\Delta\theta = 2.7°$ for three semiconducting particles and $\alpha = 0°$, while for $\alpha = 90°$ and two semiconducting and one metallic particles $\Delta\theta = 16.9°$. For case of two metallic and one semiconductor particles the minimum at $\theta_0 = 90°$ is absent, as we already mentioned from the analysis of spectral dependencies. The highest selectivity ($\Delta\theta$ below $1°$) is expected for three semiconducting

possible, since all of them have suitable potential wells at 655, 615, 685 and 710 nm, correspondingly. The accuracy of positioning the adjoining particle at the desired angle $\theta_0$ can be found from dependence of interaction energy of adjoining particle with two aggregated particles on the angle $\theta$ in the vicinity of

Table 1
Angular widths $\Delta\theta$ and potential well depths for different particle sets, different particle configurations $\theta_0$, and different light polarizations $\alpha$.

| $\theta_0$ | | mms | | ssm | | sss | |
|---|---|---|---|---|---|---|---|
| | | $\alpha = 0°$ | $\alpha = 90°$ | $\alpha = 0°$ | $\alpha = 90°$ | $\alpha = 0°$ | $\alpha = 90°$ |
| $0°$ | $\Delta\theta$ | $7.38°$ | – | $12.46°$ | – | $4.718°$ | – |
| | $|W_{min}|$ | $4.117$ | – | $20.84$ | – | $112.7$ | – |
| $90°$ | $\Delta\theta$ | – | – | – | $16.89°$ | $2.739°$ | $1.031°$ |
| | $|W_{min}|$ | $0.591$ | $5.47$ | $1.41$ | $6.49$ | $10.04$ | $61.2$ |
| $120°$ | $\Delta\theta$ | $3.44°$ | – | – | $2.1°$ | $0.19°$ | $0.22°$ |
| | $|W_{min}|$ | $1.634$ | $23.35$ | $1.311$ | $5.411$ | $41.55$ | $71.84$ |

particles, both for $\alpha = 90°$ and $\alpha = 90°$. The summary of values $\Delta\theta$ and corresponding potential well depths $|W_{min}|$ (in kT units) for two metallic and one semiconductor particles (mms), two semiconductor and one metallic particles (ssm) and three semiconductor particles (sss) is presented in Table 1, for laser intensity $10^6$ W/cm$^2$. As can be seen, for $(\alpha = 90)$ stable configurations with $\theta = 0°$ do not exist for all particle sets, in view of potential well absence throughout all considered wavelengths. For mms set, for both $\alpha = 90°$ and $\alpha = 0°$, and for ssm set and $\alpha = 0°$ the configuration $\theta_0 = 90°$ possesses potential wells, but stable configurations are absent, as well as for mms90 and ssm0 for $\theta_0 = 120°$.

Of course, values $\Delta\theta$ depend not only on the structure configuration, but as well on the intensity of laser radiation, decreasing on the increase of the latter. Joint consideration of spectral and angular widths of potential wells allows to evaluate the possibility of light-controlled formation of corresponding nanostructures.

## 4. Conclusion

In conclusion, we theoretically consider the possibility of laser-controlled formation of heterogeneous structures with required geometry containing semiconductor and metallic nanoparticles. The geometry of the structure is governed by frequency and polarization of laser radiation. Evidently, proper choice of these characteristics allows to control the geometry of the structures with larger number of particles.

## Acknowledgements

## References

[1] J.T. Bahns, S.K.R.S. Sankaranarayanan, S.K. Gray, L. Chen, Physical Review Letters 106 (2011) 095501.
[2] S. Srivastava, A. Santos, K. Critchley, K. Kim, P. Podsiadlo, K. Sun, J. Lee, C. Xu, G.D. Lilly, S.C. Glotzer, N.A. Kotov, Science 327 (2010) 1355.
[3] J. Rodriguez, L.C. DavilaRomero, D.L. Andrews, Physical Review A 78 (2008) 043805.
[4] J. Park, W. Lu, Physical Review E 83 (2011) 031402.
[5] T. Iida, H. Ishihara, Physical Review B 77 (2008) 245319.
[6] V.V. Slabko, G.G. Khachatryan, A.S. Aleksandrovsky, JETP Letters 84 (2006) 300.
[7] A.L. Rogach (Ed.), Semiconductor Nanocrystal Quantum Dots,, Springer, Wien, NY, 2008.
[8] M. Alves-Santos, Rosa Di Felice, Guido Goldoni D, Journal of Physical Chemistry 114 (2010) 3776.
[9] N.E. Lyamkina, G.A. Chiganova, V.V. Slabko, A.M. Vorotynov, M.A. Taranova, Inorganic Materials 41 (2005) 830.
[10] Y. Zhang, C. Gu, A.M. Schwartzberg, S. Chen, J.Z. Zhang, Physical Review B 73 (2006) 165405.
[11] V.M. Shalaev, Physical Reports 272 (1996) 61.
[12] L.D. Landau, E.M. Lifshitz, The Classical Theory of Fields, Butterworth-Heinemann, 1980.
[13] E.M. Aver'yanov, JETP 81 (1995) 139.
[14] B. Luk'yanchuk, N.I. Zheludev, S.A. Maier, N.J. Halas, P. Nordlander, H. Giessen, C.T. Chong, Nature Materials 9 (2010) 707.
[15] J.Y. Yan, W. Zhang, S. Duan, X.G. Zhao, A.O. Govorov, Physical Review B 77 (2008) 165301.